Chapter 20
Based on Nanocomposite Resonant Photonic Crystal Structures for Sensing Applications

Tatiana Smirnova, Pavel Yezhov, Volodymyr Hryn, Oksana Sakhno, Volodymyr Fito, and Andriy Bendziak

Abstract The approximate theory of resonance phenomena in waveguides with volume gratings that allows obtaining analytical dependencies of the spectral position of guided-mode resonances on parameters of a waveguide structure was developed. Verification of the obtained results was carried out by the rigorous coupled-wave method (RCWA). Sensitivity of sensors based on waveguide gratings was estimated. Nanocomposite sensors were fabricated by holographic method. The characteristics of the sensor were measured. A modified method for refractive indices measurement was proposed. The sensitivity of the sensors for standard and modified measurement methods was compared. It was established that the proposed method allows increasing the sensitivity of the sensor by an order of magnitude.

Keywords Polymer nancomposite · Photonic crystals · Resonant Properties · Polymer sensors

20.1 Introduction

Detection of small amounts of toxic species and contaminants is critical for environmental monitoring, human health improvement as well as prevention of biological and chemical warfare threats. Therefore development of new highly sensitive and selective sensors has a high priority. We study photonic crystal (PC)

T. Smirnova (✉) · P. Yezhov · V. Hryn
Coherent and Quantum Optics Department, Institute of Physics of NASU, Kyiv, Ukraine
e-mail: smirnova@iop.kiev.ua

O. Sakhno
Fraunhofer Institute for Applied Polymer Research, Potsdam-Golm, Germany

V. Fito · A. Bendziak
Lviv Polytechnic National University, Lviv, Ukraine

C. Palestini (ed.), *Advanced Technologies for Security Applications*, NATO Science for Peace and Security Series B: Physics and Biophysics,
https://doi.org/10.1007/978-94-024-2021-0_20

sensors based on volume gratings recorded in a nanocomposite by a holographic method.

Periodic waveguide structures formed by periodic refractive index modulation possess the resonant phenomena termed guided-mode resonance, at which phase matching of the wave diffracted by the periodic structure with the eigenmode of the waveguide occurs. Under the resonant conditions, series of strong peaks appear in the reflection spectrum of structure. The central wavelength of these peaks can be changed by varying PC structure parameters and environment permittivity. Therefore, waveguide PC structures can be used as sensors of analytes deposited on PC surface by monitoring the resonance wavelength shift. Resonance conditions also results in the strong enhancement of the field in the waveguide and near its surface (local field). The excitation of local field can promote high enhancement of fluorescence and Raman scattering of analytes (enhancement effect). In this work, we investigate the label-free sensor using wavelength shift of resonant peaks.

The main types of polymer PC structures that are investigated now are structures with corrugated surface (e.g. [1, 6, 9, 10]). Their fabrication procedures (UV or electron beam lithography, nanoimprinting, hot or UV embossing, reactive ion etching, etc.) are complicated and rather expensive. In addition, it is difficult to achieve the homogeneity of the grating over the entire surface with the mentioned methods. Relief inhomogeneity causes spectral widening of resonance peaks, decreases of reflection coefficient and, consequently, reduces the sensitivity of the sensor.

We proposed, as an alternative, waveguide PC structures based on nanocomposites with volume periodic modulation of permittivity. This approach has a number of advantages. Volume 1D, 2D structures can be fabricated by a one-step holographic lithography method that enables the production of large-size PC structures with excellent homogeneity, easily varied symmetry and period, and flat surface. For structure fabrication, we used original photosensitive polymer-based nanocomposites containing inorganic nanoparticles (NPs) developed in the Institute of Physics (Ukraine) and Fraunhofer Institute for Applied Polymer Research (Germany) [7, 8].

The goals of our work are (i) theoretical analysis of resonant properties of volume PC structures and sensitivity of sensors on their base; (ii) fabrication of the waveguide PC structures in nanocomposite by holographic method; (iii) characterization of the label-free sensor.

20.2 Theoretical Analysis of the Resonant Properties of PC Structures: Development of the Approximate Theoretical Model

In case when a plane wave with a wavelength λ falls normally on a grating of period Λ then under waveguide resonance, in which the reflection coefficient of the grating is equal to one, the condition must be satisfied as follows:

$$\beta(\lambda_0) \cong 2\pi/\Lambda, \tag{20.1}$$

where $\beta(\lambda)$ is a constant propagation of waveguide mode for given wavelength.

Equation (20.1) is valid, because the amplitude of the grating refractive index modulation is much smaller than the average grating refractive index. However, in the case when the plane wave falls on grating at the angle θ, the condition of the waveguide resonance is written as follows:

$$\frac{2\pi}{\lambda} sin\theta \pm \frac{2\pi}{\Lambda} \cong \pm\beta(\lambda, n_a), \tag{20.2}$$

where θ is the propagation angle of the plane wave in the air, n_a is refractive index of the surrounding research medium. It should be noted that the incident wave can pass through the air, research medium, grating, substrate and again the air.

The constant propagation is about $15\mu m^{-1}$ for our waveguide parameters, consisting of the grating, substrate and researched medium. The difference between the right and left parts of Eqs. (20.1) and (20.2) is less than 0.001.

Let's expand the right part of Eq. (20.2) near the point λ_0 into the Taylor series; as a result we obtain the next equation:

$$\beta(\lambda) = \beta(\lambda_0) + \frac{d\beta}{d\lambda}\delta\lambda + \frac{1}{2}\frac{d^2\beta}{d\lambda^2}(\delta\lambda)^2 + \ldots \tag{20.3}$$

We abridged ourselves to the three terms of the constant expansion of the expansion and substitute the Eq. (20.3) into (20.2) as follows:

$$\frac{2\pi}{(\lambda_0 + \delta\lambda)} sin\theta \pm \frac{2\pi}{\Lambda} = \pm\left[\beta(\lambda_0) + \frac{d\beta}{d\lambda}\delta\lambda + \frac{1}{2}\frac{d^2\beta}{d\lambda^2}(\delta\lambda)^2\right] \tag{20.4}$$

Taking into account Eq. (20.1), finally it was obtained:

$$\frac{2\pi}{(\lambda_0 + \delta\lambda)} sin\theta = \pm\left[\frac{d\beta}{d\lambda}\delta\lambda + \frac{1}{2}\frac{d^2\beta}{d\lambda^2}(\delta\lambda)^2\right]. \tag{20.5}$$

The analysis of the Eq. (20.5) allows us to conclude that, in the case of the deviation of the incident plane wave from the normal to the angle θ, there are two resonant peaks. The one is at the wavelength shorter than λ_0 and the second one is at the wavelength longer than λ_0. In fact, Eq. (20.5) splits into two equations as follows:

$$F_1(\Delta\lambda_1) = \frac{2\pi}{(\lambda_0 + \delta\lambda_1)} sin\theta - \left[\frac{d\beta}{d\lambda}\Delta\lambda_1 + \frac{1}{2}\frac{d^2\beta}{d\lambda^2}(\Delta\lambda_2)^2\right] = 0 \tag{20.6a}$$

$$F_2(\Delta\lambda_2) = \frac{2\pi}{(\lambda_0 + \delta\lambda_2)} sin\theta + \left[\frac{d\beta}{d\lambda}\Delta\lambda_2 + \frac{1}{2}\frac{d^2\beta}{d\lambda^2}(\Delta\lambda_2)^2\right] = 0 \tag{20.6b}$$

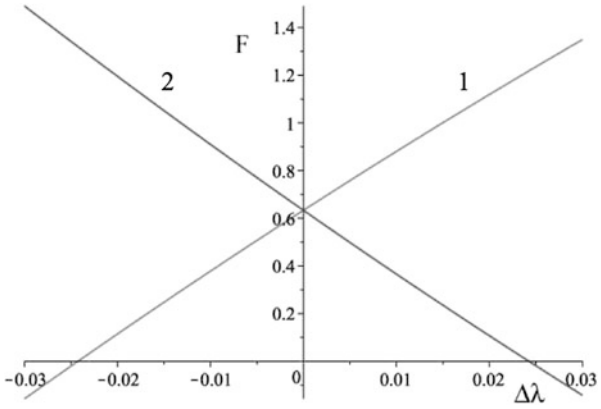

Fig. 20.1 Dependencies $F_1(\Delta\lambda_1)$ (1) and $F_2(\Delta\lambda_2)$ (2) at angle of incidence on grating is equal 3.5 angular degrees

Equations (20.6a) and (20.6b) are convenient to solve graphically. The first and second derivatives will be founded by numerically from the solution of the waveguide equation using the method described in Ref. [2]. The periodic structure was created with the following parameters: the average grating refractive index of 1.525, the refractive index of the glass substrate of 1.515, the modulation of the refractive index of the grating medium of 0.017, the grating thickness of 1.3 μm, the grating period of 0.395 μm. The resonant wavelength is 0.6053418 μm for these parameters at the normal incidence. Thus, the first $d\beta/d\lambda$ and the second derivatives are equals $-26.158647765\ \mu m^{-2}$ and $86.637\ \mu m^{-3}$ for this wavelength, respectively. The dependences $F_1(\Delta\lambda_1)$ and $F_2(\Delta\lambda_2)$ are shown in Fig. 20.1, where the roots of Eqs. (20.6a) and (20.6b) are determined by the intersection of the curves with the abscissa.

Thus, we obtained $\Delta\lambda_1 = -0.0242603\ \mu m$ and $\Delta\lambda_2 = 0.0242637\ \mu m$. Therefore, the predicted resonance wavelengths are equal $\lambda_1 = \lambda_0 + \Delta\lambda_1 = 0.5810815\ \mu m$, $\lambda_2 = \lambda_0 + \Delta\lambda_2 = 0.6296055\ \mu m$, respectively. The wavelengths calculated by RCWA for an infinite grating [5], at which the reflection coefficients are close to unity take values of 0.581138 and 0.629689 μm respectively. It can be seen that predicted wavelengths are very close to the wavelengths determined from the spectral dependences of the reflection coefficient calculated by RCWA when the incident beam is deviated from the normal.

The spectral dependence of reflectance (R) on wavelength at normal incidence and angle of incidence of 3.5° when n_a=1 is shown in Fig. 20.2.

The spectral half-width (full width at half-maximum) of the reflection peaks depends on the angle of incidence. The half-width of the spectrum is 0.0018 nm at zero beam incidence on the grating (the refractive index of the substrate is of 1.45) and increases to 0.0025 nm the angle of 30° in the air.

Theoretical investigations were shown that sensor sensitivity increases when the angle of incidence on the grating increases. It also increases when the refractive

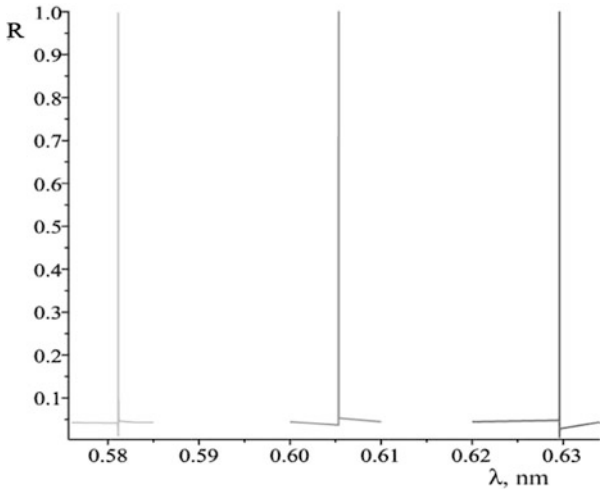

Fig. 20.2 Spectral dependencies of the reflectance (R) at the incident angles of a plane wave of 0° (central peak) and 3.5° (right and left peaks)

index of the researched medium approaches to the average grating refractive index. It was also found that PC structures with a thickness (d) of 1–2 μm, period (Λ) $\leq$ 400 nm and refractive index amplitude modulation (n_1) ≥ 0.01 are the most suitable for effective operation of the sensors.

20.3 Fabrication of PC Structures by Holographic Method

The organic inorganic UV photosensitive nanocomposite for fabrication of volume PC structures was prepared using our earlier developed technology [8]. The holographic nanocomposites are generally consisting of organic monomers of different functionality (as an organic low refractive index (n) matrix) and inorganic nanoparticles, NPs (as a high n additive). A mixture of mono-functional, isobutyl acrylate (IBA, n = 1.476) monomer and multi-functional acrylate monomer (Sartomer SR444, n = 1.481) was employed for preparation of a monomer bland using 75% wt.% IBA and 25% SR444, respectively. The photoinitiator Irgacure 1700 (Ciba) 1.5 wt.% was added to the monomer blend to provide the material sensitivity to UV (355 nm) light. The inorganic NPs series X green ($LaPO_4$ doped with rear-earth elements) from Fraunhofer Zentrum für Angewandte Nanotechnologie CAN (Hamburg, Germany) were used. The average NPs size was found of about 3–4 nm. According to the manufacturer's information the current NPs possess specific gravity of 5 g/cm^3 and the refractive index of about 1.7. The weight fraction of the inorganic core was found to be of about 85 wt.%. The concentration of the NPs

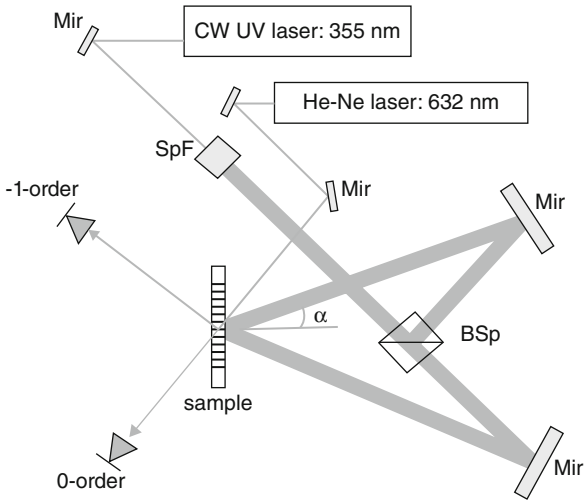

Fig. 20.3 Schematic presentation of the holographic setup: SpF-spatial filter and telescope unit, Mir – mirrors, BSp – a beam-splitter, dividing the input laser beam on two mutual recording beams

was about 25 wt.%. The fabrication method of recording layer with the thickness 1–2 μm and high film quality was developed and described in [3].

A conventional two-beam interference scheme based on an DPSS Genesis-SLM laser (Coherent) emitting at $\lambda_{rec} = 355$ nm (s-polarization) was used for holographic fabrication of PC volume structure (Fig. 20.3).

Two laser beams of about 15 mm diameter and equal intensities produce the interference pattern in the intersection plane (position "sample" in Fig. 20.3). The spatial period of the grating (Λ) was 395 nm. Because of the symmetric beam configuration, the fringes of the gratings are perpendicular to the substrates. The grating is formed due to diffusion NP redistribution in polymer matrix during exposure. The grating formation was monitored in real time by diffraction of a He–Ne laser beam (s-polarization, $\lambda_t = 633$ nm), placed at the Bragg angle corresponding to the period of the grating. The samples were exposed until the steady-state value of the diffraction efficiency was achieved (typically for 80–150 s). The recording intensity (I) of the exposing beams was varied from 10 to 50 mW/cm^2. The diffraction efficiency (η) of the grating was determined as $\eta = I_{dif}/(I_{tr} + I_{dif})$, where I_{tr} and I_{dif} are the intensity of the zero diffraction order (transmitted beam) and the first diffraction order (diffracted beam). Such estimation allows excluding the Fresnel reflection in the substrates as well as scattered light and linear absorption of the layer.

The Bragg diffraction conditions are satisfied for the gratings with the specified parameters. Only the 0^{th} and -1^{st} diffraction orders were observed in the diffraction pattern. Therefore, we used Kogelnik's formula [4] for calculation of the refractive index modulation amplitude, $n_1 = \lambda cos\theta_B asin(\eta)^{1/2}/\pi d$, where θ_B is the Bragg angle within the material, λ is the wavelength of the reading beam.

We fabricated a series of volume waveguide PC-structures, which were used for further researches. Their characteristics are follows: $d = 1.25 \div 1.70$ μm, $n_1 = 0.012 \div 0.017$.

20.4 Investigation of the Label-Free Sensor Based on the Nanocomposite PC Waveguide Structures

In order to study the properties of the sensor with volume nanocomposite PC structure a special fluid cell was fabricated. The scheme and the photo of the cell are shown in Fig. 20.4a,b. As shown in Fig. 20.4 the substrate with grating was mounted into a cell placing the grating in contact with analyte medium. The liquid was injected into the cavity of the cell with a syringe, located in the lower part of the cell. The second syringe in the upper part of the cell provided air displacement at the cuvette filling.

To change the angle of incidence the cell was installed into the goniometric stage. The halogen lamp with maximum intensity in the red part of the spectrum (of about 670 nm) was used as a light source. The spectral position of the long-wave peak in the specular reflection spectrum (the zero order diffracted beam) depending on the refractive index of the studied liquid, n_{an}, was measured.

The range of n_{an} variation for which the measurements were performed was chosen taking into account the waveguide-gratings characteristics. At $n_{an} > 1.5$, the analyte refractive index approaches the average refractive index of the waveguide-grating, n_{gr}=1.525. The system becomes unstable; the conditions for propagation of guided-modes and, correspondently, the conditions for the excitation of resonances are violated. The interaction of liquids with PC gratings was previously investigated. Only such liquids were selected, which in direct contact with the grating for 4 hours did not lead to the destruction of the grating or to the change of its parameters (diffraction efficiency, thickness).

It was found from theoretical estimation that the sensitivity of the sensor, defined as $S = \Delta\lambda/\Delta n$, increases with increasing angle of incidence. In addition, the long-wave resonance is more sensitive to the changes in the refractive index than the short-wave one, *i.e.* the spectral shift of the long-wave resonance peak, when

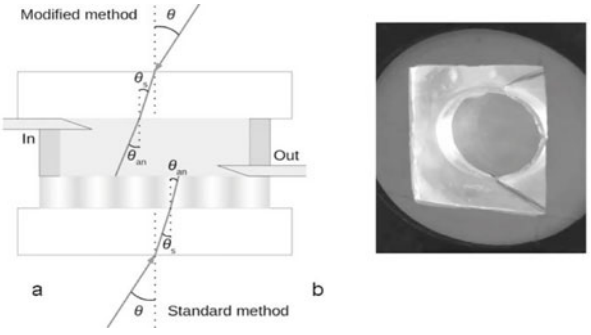

Fig. 20.4 Fluid cell construction with beam propagation (**a**), and photo of the cell (**b**). Standard method: θ = constant, θ_{an} varies for different analytes. Modified method: θ_{an} = constant, θ varies for different analytes θ_s is the angle in substrate

the refractive index changes, exceeds the shift of the short-wave peak. Therefore, the following measurements conditions were chosen for experimental studies. For different analytes the wavelength of the long-wave peak in the reflection spectrum was determined. The only difference of the observed specular reflection spectra for different analytes was the position of the resonance peaks. The half-width of the resonance peaks in all cases did not exceed 0.012 nm. The reflection coefficients were varied in the range of 10–15%. It should be noted that the value of the reflection coefficient is not fundamental by measuring the refractive indices of analytes.

In the first case light irradiation with TE polarization entered the cell from the side of a substrate, on which the PC grating is located (standard measurements). The angle of incidence in air, θ, was 20°. The dependences of λ_{res} on n_{an} were measured and theoretically calculated. There is a good agreement of the measurement results with theoretical ones. The $\lambda_{res}(n_{an})$ dependence is nonlinear, so the sensitivity of the sensor, $\Delta\lambda_{res}/\Delta n_{an}$, depends on the refractive index of the analyte and increases when its value approaches the average refractive index of the grating. The defined sensor sensitivity in this case varies within 0.4÷12 nm/RIU. One pixel shift in the peak position corresponds to a shift of 0.012 nm, which can be measured with our measurement system. As a result, a minimum detectable change in the refractive index, Δn_{min}, also varies in a range 0.0279 ÷ 0.001 RIU.

The sensitivity of sensor can be increased by modifying the measurement procedure. If the radiation enters the cell from the side of test analyte, by changing the angle of incidence θ, it is possible to measure the resonance wavelength at a constant angle θ_{an} of the radiation propagation in analytes with different n_{an}. The theoretically calculated dependences of the resonance wavelength on the refractive index of the medium for different θ_{an} shown that in this case the sensitivity of the measurements also arises with increasing θ_{an}. Herewith a long-wave reflection peak is more sensitive to n_{an} changes.

In the pointed range of n_{an}, the dependence $\lambda_{res}(n_{an})$ can be approximated by a straight line Fig. 20.5. The slope of this line determines the sensitivity of sensor. When $\theta_{an} = 15°$ and $1 \leq n_{an} \leq 1.5$, the range of θ is $1° \div 22.844°$. It corresponds to the spectral range of long-wave resonances of 708.344 nm ÷ 761.730 nm. By calculating the value of θ for each of analyte and measuring the reflection spectra for each θ, we determined the corresponding values of λ_{res} for long-wavelength peaks. The measurement results are shown in Fig. 20.5.

There is a coincidence of the measured values with the calculated theoretically. It confirms clear the applicability of the presented method. The defined value of S is equal to 122 nm/RIU. The minimum detectable change in the refractive index, Δn_{min}, was found as 1×10^{-4} RIU. It is important to note that this limitation is determined by the detection system used. The theoretical limit of the refractive index change is predicted to be two orders of magnitude lower.

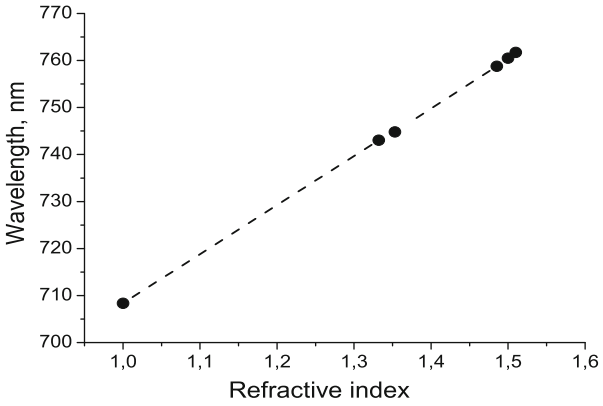

Fig. 20.5 Experimentally measured spectral positions of resonance peaks (circle dots) obtained for the angle in liquid 15° and dependence of resonance wavelength on refractive index calculated by RCWA method (dash line)

20.5 Conclusions

Approximate methods for determining the parameters of the created grating as sensitive sensor element for measuring the refractive index of the research medium has been developed. It is possible to calculate the resonance wavelengths for different angles of incidence using obtained approximate equations and knowing λ_0.

The exact values of the resonant wavelengths at different angles of the incidence on the grating were found by the RCWA method. They are very close to the obtained values of wavelengths using developed approximate method.

Suitable organic-inorganic nanocomposites were prepared. Optimization of the exposure conditions allows obtaining the PC structures with thickness $<2\,\mu$m and the refractive index amplitude modulation $0.01 \div 0.017$.

The characteristics of the sensor based on nanocomposite PC waveguide structure were examined. A modified measurement method was proposed. The modified method provides the sensor sensitivity 122 nm/RIU and minimal detectable change in the refractive index Δn_{min} of about 1×10^{-4} RIU.

Acknowledgments This work was supported by the grant in the framework of the a Multi-years Project from the SPS Programme – SPS G5351 "Science for Peace and Security" "Nanocomposite Based Photonic Crystal Sensors of Biological and Chemical Agents" (Project 12/18-52).

References

1. Chaudhery V, George S, Lu M, Pokhriyal A, Cunningham BT (2013) Nanostructured surfaces and detection instrumentation for photonic crystal enhanced fluorescence. Sensors 13:5561–5584
2. Fitio VM, Romakh VV, Bobitski YV (2014) Numerical method for analysis of waveguide modes in planar gradient waveguides. Mater Sci (Medžiagotyra) 20:256–261
3. Hryn V, Sakhno O, Bendziak A, Fito V, Yezhov P, Smirnova T (2019) Development of the waveguide photonic crystal structures formed by distribution of nanoparticles in polymer matrix. In: Fesenko O, Yatsenko L (eds) Nanophotonics, Nanooptics, Nanobiotechnology, and Their Applications. NANO 2018. Springer Proceedings in Physics, vol 222. Springer, Cham, pp 73–85
4. Kogelnik H (1969) Coupled wave theory for thick hologram gratings. Bell Syst Tech J 48:2909–2947
5. Moharam MG, Gaylord TK (1983) Rigorous coupled-wave analysis of grating diffraction – e-mode polarization and losses. J Opt Soc Am 73:451–455
6. Nair RV, Vijaya R (2010) Photonic crystal sensors: an overview. Prog Quantum Electron 34:89–134
7. Sakhno OV, Goldenberg LM, Stumpe J, Smirnova TN (2009) Effective volume holographic structures based on organic-inorganic photopolymer nanocomposites. J Opt A Pure Appl Opt 11:024013
8. Sakhno OV, Smirnova TN, Goldenberg LM, Stumpe J (2008) Holographic patterning of luminescent photopolymer nanocomposites. Mater Sci Eng C 28:28–35
9. Yaremchuk I, Tamulevičius T, Fitio V, Gražulevičiūte I, Bobitski Y, Tamulevičius S (2013) Guide-mode resonance characteristics of periodic structure on base of diamond-like carbon film. Opt Commun 301–302:1–6
10. Zhuo Y, Cunningham BT (2015) Label-free biosensor imaging on photonic crystal surfaces. Sensors 15:21613–21635